Evolution in Electrical and Electronic Engineering Vol. 3 No. 2 (2022) 676-686

EEEE

Homepage: http://publisher.uthm.edu.my/periodicals/index.php/eeee
e-ISSN : 2756-8458

Rotor-Pole Number Analysis of Double Stator PM-FSM Using 2D FEA For Optimal Output Performances

Mohamad Zakwan Mohd Dzubaidi[1], Md Zarafi Ahmad[1]*

[1]Faculty of Electrical and Electronic Engineering,
Universiti Tun Hussein Onn Malaysia, Batu Pahat, 86400, MALAYSIA

*Corresponding Author Designation

DOI: https://doi.org/10.30880/eeee.2022.03.02.080
Received 13 July 2022; Accepted 13 September 2022; Available online 30 October 2022

Abstract: Recently, most reported research on Flux Switching Motor (FSM) are focused on Single Stator Permanent Magnet (PM) FSM topology in which the excitation sources of PMs and armature coils are accommodated at the stator. Then, there is reported research on double-stator 6Slot-7Pole configuration and shows good improvement in the output performances. However, no slot-pole number analysis has been carried out to perform the best motor configuration for optimal output performances. Thus, in this project, 12Slot-10Pole and 12Slot-14Pole DS-PMFSM analysis is carried out and then compared with 6Slot-7Pole. The analyses are implemented based on two-dimensional (2D) finite element analysis (FEA) which uses JMAG-Designer software. The concerned performance parameters are motor flux linkage, cogging torque back-emf, flux distribution, output torque and power. The results obtained show that 12Slot-14Pole DS-PMFSM gets the better result for cogging torque which is 1.076Nm, output torque at 36.8116Nm, back-emf at 2.434, flux linkage, and flux distribution than the results for 12Slot-14Pole DS-PMFSM for cogging torque which is 2.999Nm, output torque at 5.484Nm, back-emf at 2.252, flux linkage, and flux distribution. Thus, it is concluded that the investigation for slot-pole number had successfully performed the best configuration of the motor.

Keywords: DS-PMFSM, Rotor-Pole, Segmental Rotor, Output Performance

1. Introduction

Industrial motor manufacturers have been promoting the use of electrical motors for industrial and transportation needs in recent years. Many industries that employ electric motors for a variety of purposes have boosted their demand for motor manufacturing services. The use of an electrical motor in a wind turbine, for example, must be compatible with the power capacity and electrical motor size required by the wind turbine idea [1]. Aside from that, electrical machine drives, especially AC drives, need to be more efficient because of the global trend toward energy conservation. New energy-efficient, high-performance electric drives that utilize contemporary PM brushless or synchronous motors have been made possible by recent developments in permanent magnet (PM) materials, solid-state

*Corresponding author: zarafi@uthm.edu.co

technology, and microelectronics. Due to rare-earth PMs, these motors outperform asynchronous motors in terms of efficiency, power factor, power density, and dynamic performance without compromising dependability [2].

Since the high torque densities are a result of the bipolar flux and flux links used in flux-switching devices. Segmental rotor use considerably affects the flux switching scheme compared to toothed rotor use but allows for the deployment of radially acting magnets in the stator teeth. The entire setup offers benefits like fault tolerance, brushless operation, simple construction, and easy cooling [3]. Due to a more robust usage of the motor's interior area, the design finally boosted torque density. The significant number of excitation sources on the stator will also limit the armature area, resulting in poor temperature conditions and low torque density [3].

Because the DS-PMFSM is a combination of two separate motors, it can be employed in various operating modes for different working cycles. When the vehicle is moving at a modest speed, the external motor can run independently. On the other hand, the internal engine can achieve high rates while working at cruising speed. Under heavy loads or climbs, the interior and exterior motors must work together to provide additional power. As a result, DSPM is being considered a suitable candidate for HEV applications. This study aims to improve the performance of the segmental rotor DS-PMFSM by combining the stator slot and rotor pole numbers of the DS-PMFSM, which are 6S-7P and 12S-10P respectively. Figures 1 shows the three-phase 12S/6P FEFSM (segmented rotor).

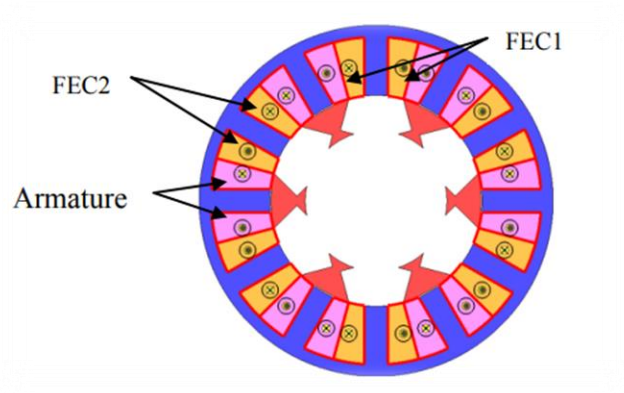

Figure 1: Three-phase 12S/6P FEFSM (segmented rotor)

2. Methodology

There are numerous procedures that must be completed in order to successfully complete the project and accurately forecast that the project scope is met. This chapter discusses how to design and analyse a double stator permanent magnet flux switching motor (DS- PMFSM) using JMAG-Geometry Editor and JMAG-Designer version 17.1, which is a 2D-Finite Element Analysis supplied by Japan Research Institute (JRI). The inner stator, outer stator, permanent magnet, rotor, and armature are all designed using the JMAG-Geometry Editor. After that, the design will be analysed in JMAG-Designer to complete the machine's operating principle, coil test, flux strengthening, back-emf, cogging torque, flux line, flux distribution, no load, and load test analysis.

2.1 Design specifications of the initial design

The initial design restriction is illustrated in Table 1 and Figure 2 demonstrates the structure of 6S-7P segmental rotor DS-PMFSM. The maximum of armature current density, JA is set at 30 Arms/mm2, respectively. The electrical Nippon steel 35H210 material is used for the stator and rotor body. While,

stator outer diameter, rotor outer diameter, and air gap are restricted to 96 mm, 59 mm, and 0.5 mm, respectively. Table 1 shows the parameter of the DS-PMFSM design.

Table1. Parameter of DS-PMFSM design

Parameter	Value
Phase	3
Stator pole/slot number	6
Rotor pole number for inner and outer	7
Outer stator outer radius (mm)	112
Outer stator inner radius (mm)	79
Inner stator outer radius (mm)	44.8
Air gap length (mm)	0.6
Rotor outer radius (mm)	78.4
Rotor inner radius (mm)	45.4
Shaft Radius (mm)	11.2
Armature coil turns for outer stator	139
Armature coil turns for outer stator	37
Stack length (mm)	75
Stator tooth width (mm)	6.6
Rotor speed (rpm)	1000
Max power (kW)	5.66
Cogging torque (Nm)	1.14
Max current (A)	50
Max torque (Nm)	32.88

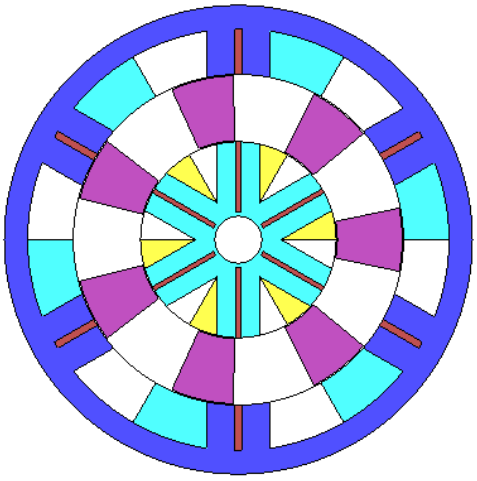

Figure 2: The initial design of the 6S-7P segmental rotor DS-PMFSM

3. Performance of Initial Design of PMFSM

3.1 6 Coil Arrangement Test of DS-PMFSM

Coil testing configuration at no load for the DS-PMFSM segmental rotor proves the operational concept and positioning of armature coils in their particular slots. In a balanced three-phase (3), system, three phases of 6 coils are recognised by evaluating a magnetic flux connection on each coil. To begin, each armature coil is examined using the six coil arrangement test. The goal of this approach is to figure out how each armature coil forms a flux linkage pattern. With the same pattern, the flux linkage is gathered together. According to the results of the test, two coils from a 6-armature coil flux linkage will create identical DS-PMFSM configuration patterns for the inner and outer stators, as shown in Figure 3.

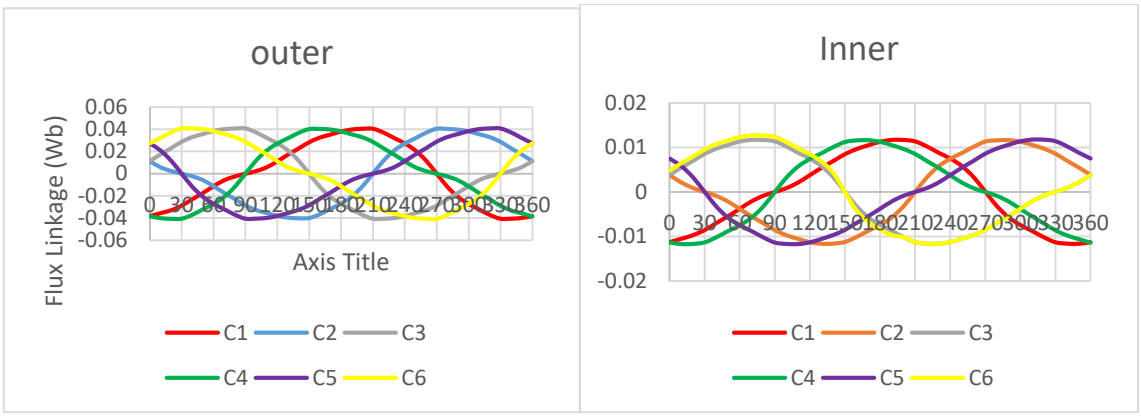

Figure 3: Result of 6S-7P coil arrangement test

3.2 U, V, W Test

The 3-flux linkage indicates the polarity and phase of the entire armature coil. According to the figure, the resultant amplitude of the flux created by PM is roughly 0.076 Wb for the outer stator and 0.023 Wb for the inner stator, which is suitable for motor function. The armature's waveform is sinusoidal, supporting the DS-functioning PMFSM's concept. The armature coil test for the inner and outer stator DS- PMFSM is shown in Figure 4.

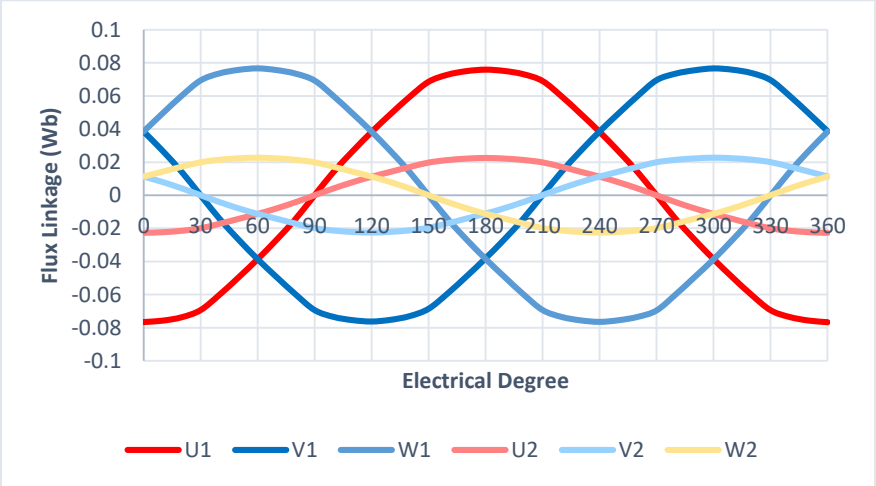

Figure 4: Flux linkage of SegR. 6S-7P DS-PMFSM

3.3 Cogging torque

Cogging torque, also known as a detent or 'no current' torque, is an unwanted torque in which the peak-to-peak value must be less than 10% of the average torque, or else the motor structure will generate vibration, acoustic noise, and poor efficiency performance, resulting in motor damage. Figure 5 depicts the graph of PM-produced cogging torque for six and twelve cycles with no current applied to the armature current density and Ja set to 0Arms/mm2. Furthermore, the greatest peak-to-peak cogging torque is roughly 1.5Nm peak-to-peak, as shown in the graph. The proposed design offers a low cogging torque, which is advantageous for machine operation.

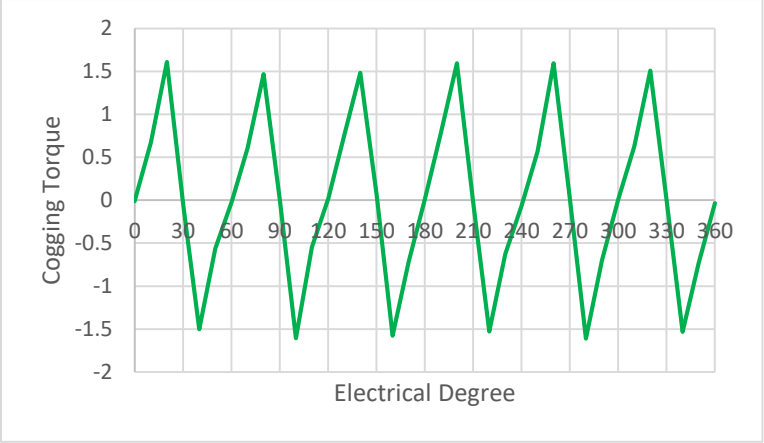

Figure 5: Cogging torque for initial 6S-7P SegR. DS-PMFSM

3.4 Induced Voltage

The back electromagnetic force (EMF) on a 6S-7P DS-PMFSM segmental rotor is investigated further at 1000rpm when no load is applied. Figure 6 shows the findings of the back EMF for the inner and outer stators. The flux source of the permanent magnet yielded induced voltage 6S-7P DS-PMFSM of inner and outer with amplitudes of 29.58V and 102.425.

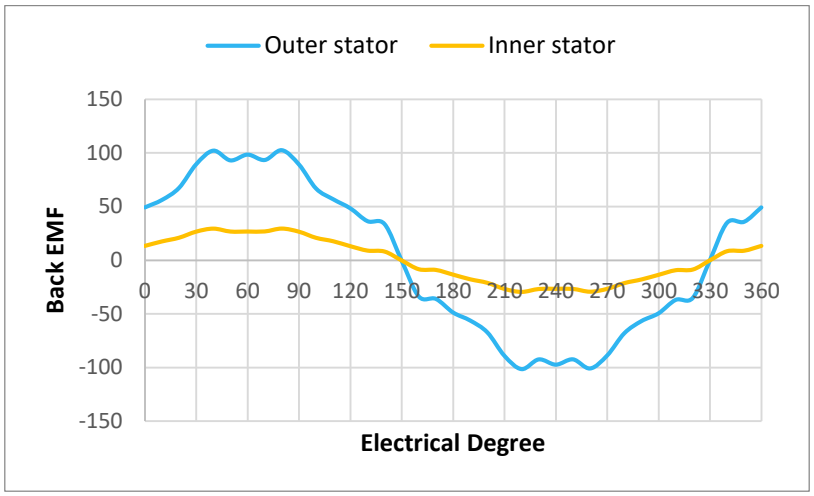

Figure 6: Back EMF for initial 6S-7P SegR. DS-PMFSM

3.5 Flux Line Analysis

The purpose of flux lines is to observe the flux flow. Figure 7 demonstrates that all flux lines move from the inner stator teeth to the rotor poles to the outer stator and bounce back to the neighbouring rotor poles to complete entire cycles. Furthermore, the majority of the flux is dispersed and saturated at the excitation stator and PM, which are the outer and inner stators, respectively. However, excessive flow leakage in the motor could result in a massive volume of flow into a rotor with a high gap flow density. Furthermore, excessive extra flux into the rotor could result in a larger back-emf. Figure 7 illustrates the flux path of the proposed twin stator PMFSM system.

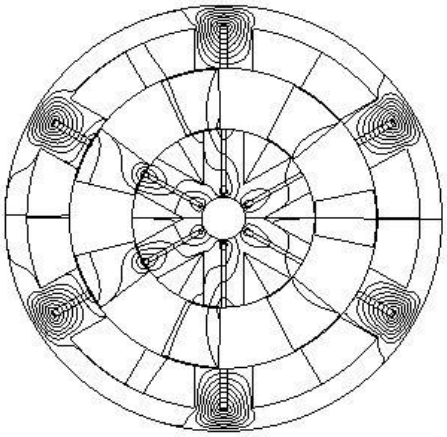

Figure 7: Flux line for initial 6S-7P SegR. DS-PMFSM

3.6 Flux Distribution Analysis

The impact of flux saturation in the machine is indicated by the function of flux line distribution. The highest magnetic flux density of the 6S-7P DS-PMFSM design with Ja 0 Arms/ mm² was 2.548Wb, while the lowest value was 0.0000006302 Wb, as shown in Figure 8, which also shows the flux density distribution.

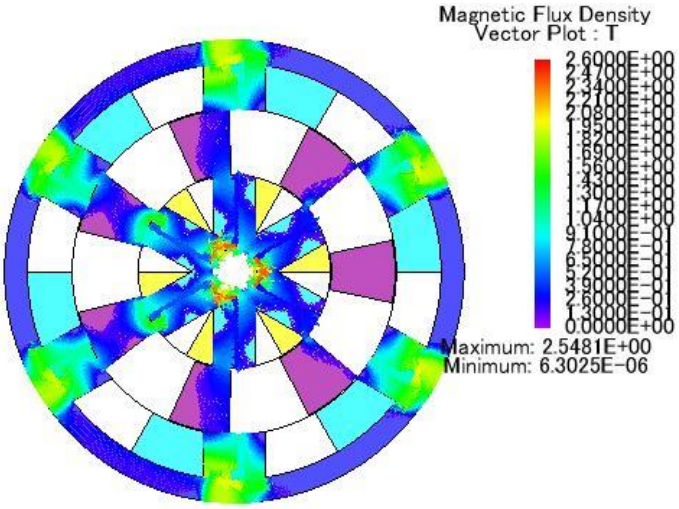

Figure 8: Flux Distribution for initial 6S-7P SegR. DS-PMFSM

3.7 Load Test Analysis

The motor's capability is defined by its performance when the maximum current density Ja is injected into it. Figure 9 shows the average torque production vs. the armature current density, Ja, for the motors under discussion. Then Ja is changed from 5 to 30 Arms/mm², which has an effect on torque performance. Torque rises in lockstep with Ja, but when a big Ja value is injected, torque climbs slightly due to production-related flux saturation. The maximum torque density for 6S-7P is approximately 11.92Nm/kg at maximum armature current densities of Ja, 30 Arms/mm².

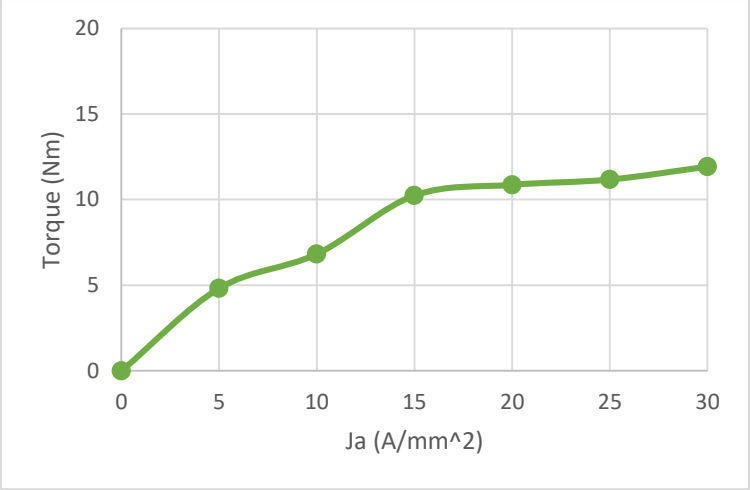

Figure 9: Torque vs armature current density, Ja for initial 6S-7P SegR, DS-PMFSM

4. Investigation of the Proposed Segmental Rotor Structure DS-PMFSM

The methods used to achieve the study's first goal are described in this section. The main goal is to design and determine the capability of the 6 stator slots and 7 segmental rotor poles of DS-PMFSM, then redesign for 12 stator slots and 10 segmental rotor poles and 12 stator slots and 14 segmental rotor poles. It is vital to conduct tests to discover the operating principle in order to ensure that the motor will run smoothly while developing a new structure. The machine design procedure is depicted in Figure 10, and the overall research findings are as follows.

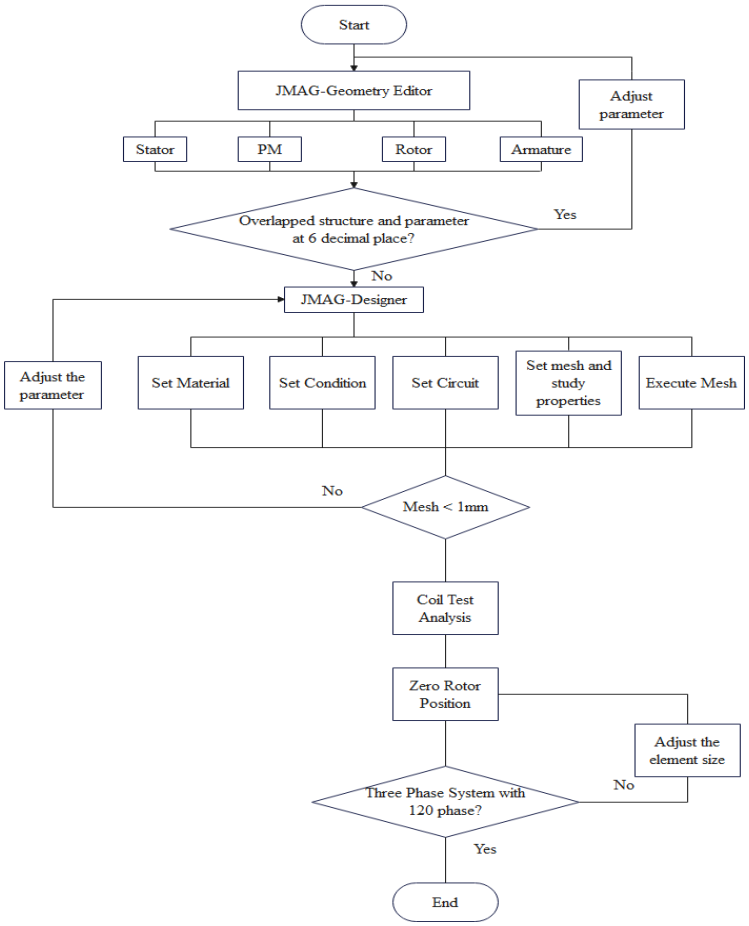

Figure 10: The overall process design and analysis flowchart

4.1 Result of Flux Linkage

Coil testing configuration at no load for the DS-PMFSM segmental rotor proves the operational concept and positioning of armature coils in their particular slots. In a balanced three-phase (3), system, three phases of 12 armature coils are recognised by evaluating a magnetic flux connection on each coil. To begin, each armature coil is examined using the six coil arrangement test. The goal of this approach is to figure out how each armature coil forms a flux linkage pattern. With the same pattern, the flux linkage is gathered together. According to the results of the test, four coils from a 12-armature coil flux linkage will create identical DS-PMFSM configuration patterns for the inner and outer stators, as shown in Figure 11 and Figure 12.

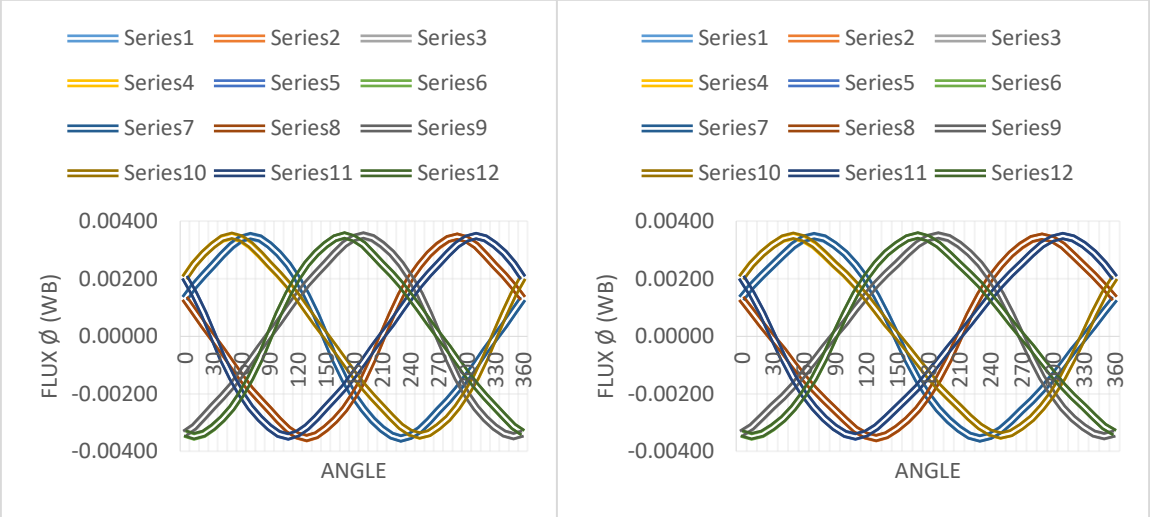

Figure 11: Flux linkage of SegR. 12S-10P DS-PMFSM

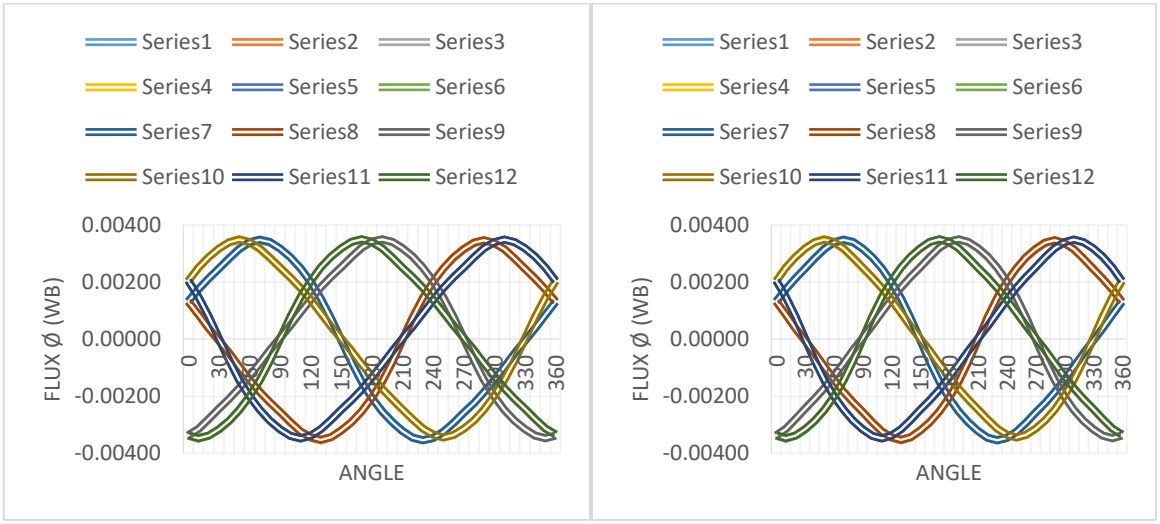

Figure 12: Flux linkage of SegR. 12S-14P DS-PMFSM

4.2 Result of Cogging Torque

Cogging torque, also known as a detent or 'no current' torque, is an unwanted torque in which the peak-to-peak value must be less than 10% of the average torque, or else the motor structure will generate vibration, acoustic noise, and poor efficiency performance, resulting in motor damage. Figure 13 and Figure 14 depict the graph of PM-produced cogging torque for twelve cycles with no current applied to the armature current density and Ja set to 0Arms/mm2. Furthermore, the greatest peak-to-peak cogging

torque is roughly 1.5Nm peak-to-peak, as shown in the graph. The proposed design offers a low cogging torque, which is advantageous for machine operation.

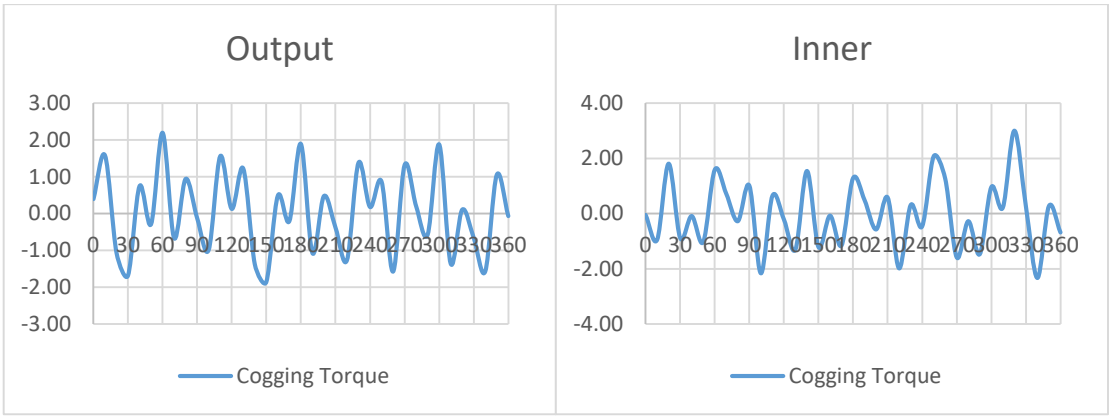

Figure 13: Cogging torque of SegR. 12S-10P DS-PMFSM

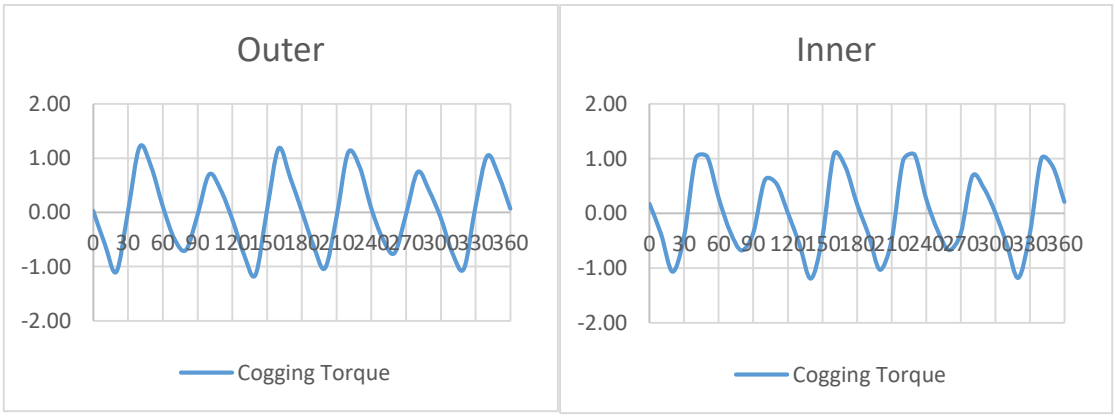

Figure 14: Cogging torque of SegR. 12S-14P DS-PMFSM

4.3 Result of Induced Voltage

The back electromagnetic force (EMF) on the segmental rotor is investigated further at 1000rpm when no load is applied. Figure 15 and Figure 16 show the findings of the back EMF for the inner and outer stators. The flux source of the permanent magnet yielded induced voltage 12S-10P DS-PMFSM of inner and outer yielded 2.252V and 1.416V and 12S-14P DS-PMFSM of inner and outer yielded 2.434V and 3.572V.

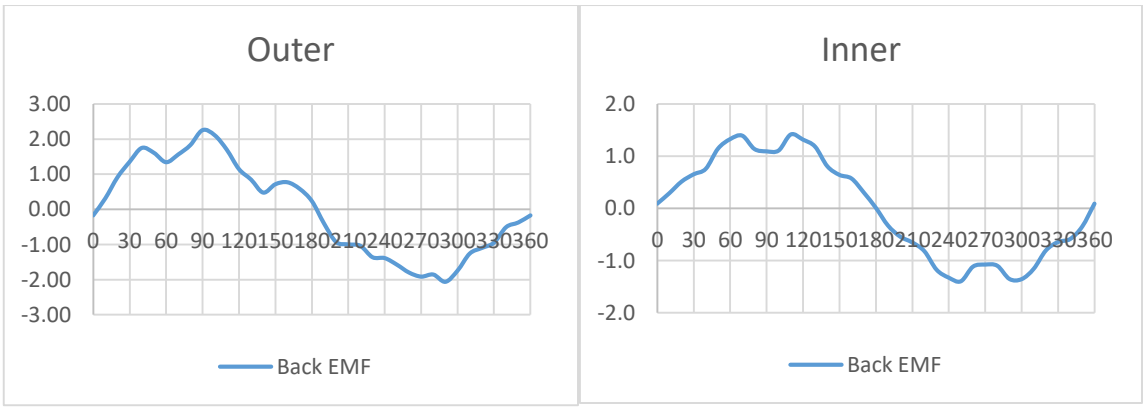

Figure 15: Induced voltage for 12S-10P DS-PMFSM

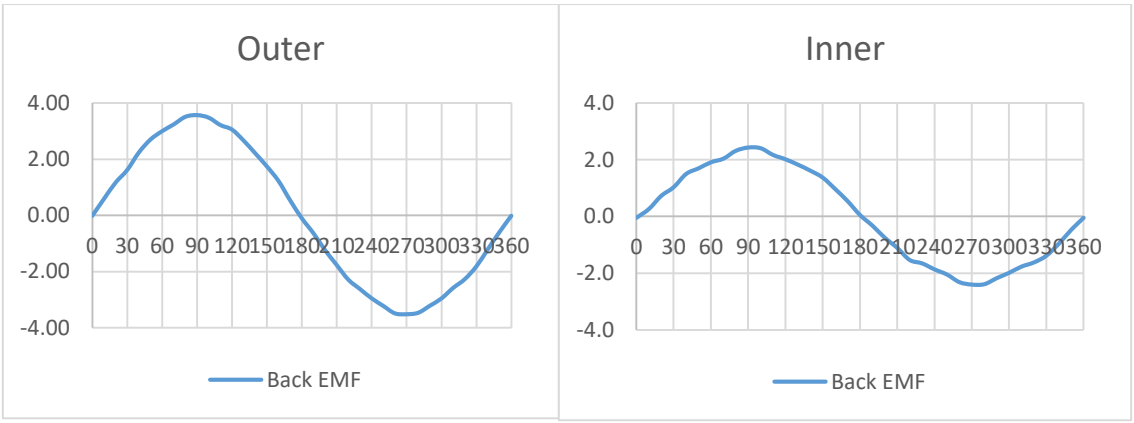

Figure 16: Induced voltage for 12S-14P DS-PMFSM

4.4 Load Test Analysis

The motor's capability is defined by its performance when the maximum current density Ja is injected into it. Figure 17 and Figure 18 show the average torque production vs. the armature current density, Ja, for the motors under discussion. Then Ja is changed from 5 to 30 Arms/mm², which has an effect on torque performance. Torque rises in lockstep with Ja, but when a big Ja value is injected, torque climbs slightly due to production-related flux saturation. The maximum armature current densities of Ja, 30 Arms/mm², the greatest torque density attained by 12S-10P is 5.48Nm/kg and for 12S-14P is 36.8116Nm/kg. No load investigation yielded a cogging torque of 1.5Nm. For the original DS-PMFSM, the cogging torque to output torque ratio is 12 percent. Furthermore, the plotted graph shows that no saturation occurs, and no torque decreases in response to the current density field, implying that design improvement and optimization will enhance torque beyond target.

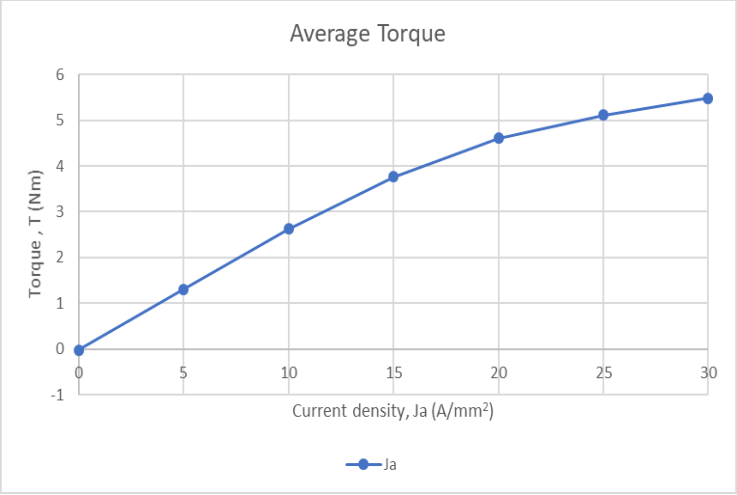

Figure 17: The graph of torque versus JA for 12S-10P DS-PMFSM

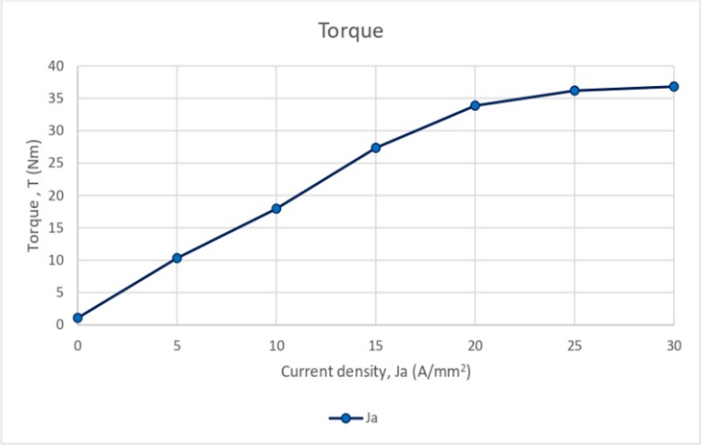

Figure 18: The graph of torque versus JA for 12S-14P DS-PMFSM

5. Conclusion

The design and investigation of the segmental rotor DS-PMFSM are provided in this project. To begin, the proposed machine's design procedure has been thoroughly defined. The models were then put through a coil arrangement test to confirm each armature coil phase and verify the machinery's working concept. The cogging torque, back-emf, flux line, and flux distribution of the recommended DS-PMFSM design were investigated for no-load conditions. In addition, load tests were performed to assess the machine's initial performance. Based on the findings, it can be inferred that the machine's initial implementation can be further enhanced by design refinement and optimization processes, resulting in more excellent output performance. In conclusion, it can be stated that the 12S-14P DS-PMFSM motor has better output performance than the 12S-10P motor in terms of torque output which is 36.8116Nm, compared to the 12S-10P motor, which is capable of producing 5.4838Nm. In addition, the 12S-14P motor can also reduce the cogging torque to 1.076Nm compared to the 12S-10P motor, which creates a higher cogging torque of 3.0Nm. It is not suitable for motors and can provide interference to the motor. However, the 6s-7p produces more high torque output than the 12s-10p with 11.9204Nm and produces lower cogging torque than the 12s10p motor which is 1.611Nm. Finally, the initial objective of designing and analyzing the performance of a three-phase 6S/7P, 12S/10P, and 12S14P segmental DS-PMFSM rotor for this Final Year Project was completed.

Acknowledgement

The authors would like to thank the Faculty of Electrical and Electronic Engineering, Universiti Tun Hussein Onn Malaysia for its support.

References

[1] Li, S., Li, Y. J. & Sarlioglu, B. (2015). Performance assessment of high- speed flux switching permanent magnet machine using ferrite and rare earth permanent magnet materials. Electric Power Components and Systems. pp. 711– 720.

[2] J.F. Gieras, M. Wing, Permanet Magnet Motor Technology, ISBN:0-8247-9794-9, Marcel Dekker, New York, 1997.

[3] A. M. B. C. &. A. M. Zulu, "Permanent magnet flux switching synchronous motor employing a segmental rotor," IEEE Transactions on Industries. 6., pp. pp. 2259- 2267., 2012.